analytical chemistry

Article

pubs.acs.org/ac

Reactive Carbon Nano-Onion Modified Glassy Carbon Surfaces as DNA Sensors for Human Papillomavirus Oncogene Detection with Enhanced Sensitivity

Joanne P. Bartolome,[†] Luis Echegoyen,*[,‡] and Alex Fragoso*[,†]

[†]Nanobiotechnology & Bioanalysis Group, Departament d'Enginyeria Química, Universitat Rovira i Virgili, Avinguda Països Catalans 26, 43007 Tarragona, Spain

[‡]Department of Chemistry, University of Texas at El Paso, El Paso, Texas 79968, United States

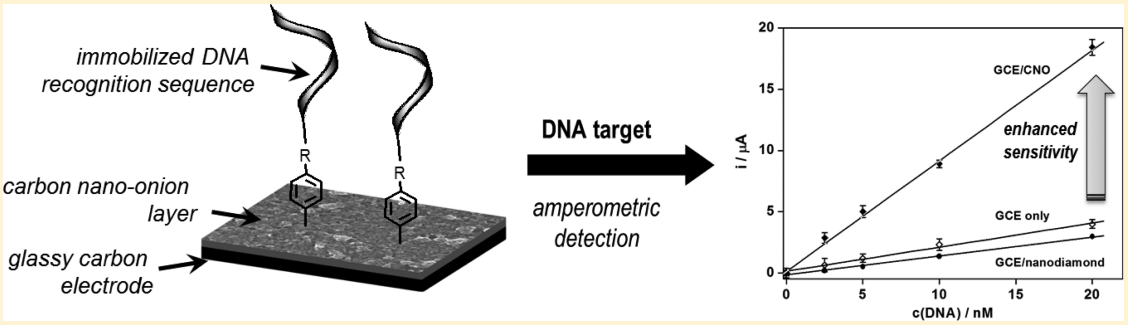

ABSTRACT: Glassy carbon electrodes were modified with small carbon nano-onions (CNOs) and activated by electrografting of diazonium salts bearing terminal carboxylic acid and maleimide groups. The CNO-modified surfaces were characterized by ESEM and AFM microscopy as well as by electrochemical techniques. The modified electrodes were used for the amperometric detection of a model DNA target sequence associated with the human papillomavirus by immobilizing short recognition sequences by amidation or thiol-maleimide reactions. The analytical parameters of the developed biosensors were compared with glassy carbon electrodes without CNOs. In both cases, the incorporation of CNOs resulted in an enhancement in sensitivity and a decrease in detection limits ascribed to a combination of large surface areas and enhanced electron transfer properties of the CNO-modified electrodes. These results offer promise for the construction of other CNO-based biomolecule detection platforms with enhanced sensitivities.

Carbon nano-onions (CNOs) were first reported by Ugarte in 1992 after irradiating a sample of carbon soot particles under an electron beam.[1] This allotrope of carbon is a multilayered fullerene concentrically arranged one inside the other. Their average sizes typically range from 5 to 40 nm in diameter,[2] and unlike other carbon allotropes, they remain relatively less explored.[3,4] Similar to other carbon nanomaterials, CNOs are generally insoluble in organic and inorganic solvents. To improve the solubility and applicability, CNOs have been chemically functionalized using a wide range of reactions including cycloadditions,[5,6] amidations,[6,7] oxidations,[8] or radical additions of diazonium compounds,[9] as well as by means of supramolecular interactions.[10,11]

CNOs have been incorporated into polydimethylsiloxane, polyurethane, and polymethyl-methacrylate matrices, and the electromagnetic properties of these materials have been investigated.[12] Plonska and co-workers have fabricated a novel type of CNO-based composite containing poly(diallyldimethylammonium chloride) (PDDA) or chitosan.[13] The composite films were deposited on glassy carbon, and the capacitance of the films was shown to be primarily related to the amount of CNOs incorporated into the layer of the filler. The low relaxation times exhibited by these composites indicate that they can operate as capacitors in short time windows. Recently, the electrochemical properties of CNO/PDDA composites deposited on gold were examined by voltammetric techniques, and their ability to detect dopamine in the presence of uric and ascorbic acids was studied.[14] CNOs have also been incorporated in microsupercapacitors[15] to exploit their fast charging and discharging rates and have been used as additives in lubricants due to their tribological properties[16] and as catalysts.[17]

More recently, some studies have focused on the possibility of using CNOs for biomedical applications[18] such as for cell imaging[19,20] and have also shown low cytotoxicity and low inflammatory properties.[21] The covalent functionalization of oxidized CNOs (containing COOH groups) with biomolecules by using biotin−avidin interactions has been reported.[22] An amino-terminated monolayer was created on a gold surface and oxidized CNOs were covalently attached by amide bonds followed by reaction of biotin hydrazide with the remaining

Received: March 9, 2015
Accepted: June 11, 2015
Published: June 11, 2015

DOI: 10.1021/acs.analchem.5b00924
Anal. Chem. 2015, 87, 6744−6751

COOH groups. This Au/CNO/biotin surface was used to capture avidin, a process that was followed by surface plasmon resonance. To the best of our knowledge, this is the only report involving the use of CNO-modified surfaces to study biomolecular interactions.

Considering the previously demonstrated importance of the incorporation of carbon nanomaterials in transducer surfaces[23,24] and the lack of reports on the use of CNOs for this purpose, we evaluate the possibility of using CNO-modified electrodes in biosensing applications. A stable dispersion of pristine CNOs was initially prepared and deposited on glassy carbon (GC) electrodes to form a mechanically stable GC/CNO surface that was further modified by electrochemical grafting of two different diazonium salts derived from 4-aminophenylacetic acid (PAA) and 4-aminophenylmaleimide (PM) (Scheme 1). The GCE/CNO/PAA and GCE/CNO/PM surfaces were evaluated as supports for the attachment of small biotinylated or thiolated DNA probes. These CNO-based biosensors were then used for the amperometric detection of human papillomavirus (HPV)[25] oncogene DNA sequences as a model system using a sandwich assay. The sensitivity and analytical performance of the developed GCE/CNO sensors were compared with those of diazonium-modified electrodes in the absence of CNOs.

Scheme 1. Strategy Employed for Modification of Glassy Carbon Electrodes with CNOs and Diazonium Salts

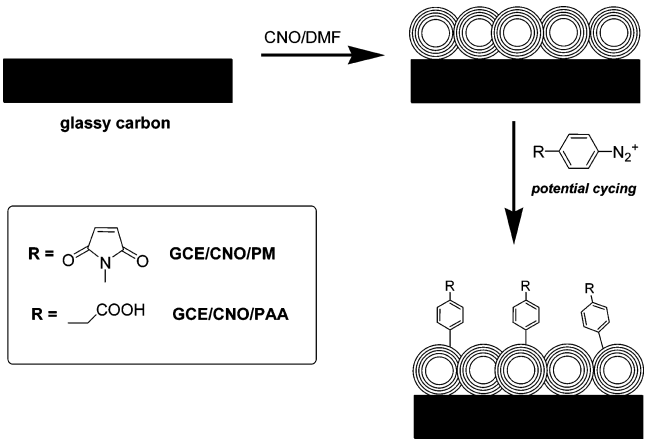

EXPERIMENTAL SECTION

Reagents. CNOs were prepared as previously reported.[6] Dimethylformamide (DMF), N-(4-aminophenyl)-maleimide, 4-aminophenyl acetic acid, $NaNO_2$, tetrabutylammonium tetrafluoroborate (TBA-TFB), 6-ferrocenyl-1-hexanethiol (Fc-SH), acetonitrile, 1-ethyl-3-[3-(dimethylamino)propyl]-carbodiimide hydrochloride (EDC), *N*-hydroxysuccinimide (NHS), streptavidin from *Streptomyces avidini*, and tetramethylbenzidine (TMB) liquid substrate for ELISA were obtained from Sigma-Aldrich and used as received. HPV16E7-related 5′-biotinylated and 5′-thiolated DNA capture probe, target sequence, and horseradish peroxidase (HRP)-labeled reporter probe (21-mer) were purchased from Biomers.net (Ulm, Germany). The nucleotide sequences of these probes can be found elsewhere.[26] All other chemicals used in buffer solution preparations were of analytical reagent grade. All solutions were prepared with Milli-Q water.

Instrumentation. A tip sonicator (amplitude 60%, cycle 0.5, Ultraschallprocessor UP200S) was used to mechanically disperse CNOs. All electrochemical measurements were obtained using a PC-controlled PGSTAT 12 Autolab potentiostat (Eco Chemie, The Netherlands) equipped with BASi C-3 Stand (RF-1085) three-electrode cell. This configuration contains a bare or modified glassy carbon electrode (BAS model MF-2012, 3.0 mm diameter) as the working electrode, a platinum wire as the counter electrode, and a Ag/AgCl(sat) as the reference electrode. Impedance spectra were recorded over the frequency range of 10 kHz-0.1 Hz at a bias potential of +0.22 V and an ac amplitude of 5 mV. Transmission electron microscope images of CNOs dispersed in DMF were obtained on a JEOL 1011 instrument using a copper grid. Environmental scanning electron microscopy (ESEM) was recorded in a Quanta 600 microscope (FEI Company, Inc.) under high vacuum at 25 kV. The modified GCEs were placed vertically in the sample chamber and analyzed at a 10 mm working distance. Atomic force microscopy (AFM) analyses were recorded using a Molecular Imaging model Pico SPM II (Pico+) instrument from Agilent Technologies in tapping mode using a 1 nm high resolution SHR150 tip from Budget Sensors. A freshly cleaved thin layer of highly oriented pyrolytic graphite (from SPI) was used as substrate.

Deposition of CNOs on GC electrodes. Prior to the deposition of CNOs, the glassy carbon electrode was polished to a mirror finish with 0.3 μM alumina slurries, cleaned, sonicated in Milli-Q water for 5 min, and then dried under a stream of nitrogen gas.

Two milligrams of purified CNOs were dispersed in 10 mL dimethylformamide (DMF) and were subjected to tip sonication for 30 min to obtain a homogeneous dispersion. To obtain a thin layer of CNOs on the surface of the electrode, the homogenized solution was sprayed onto the clean electrode for 2 s and then dried with hot air at about 150 °C (Scheme 1). The process was repeated 30 times, and after every fifth cycle, the electrode was thoroughly washed with Milli-Q water and acetone and then dried again. This method created a compact and mechanically stable layer of about 9 μm thickness as observed by ESEM.

Electrochemical Grafting of Diazonium Salts on GCE/CNO. A stirred ice-cold solution of PAA or PM (2 mL, 10 mM) in 0.5 M HCl was treated with 2 mL of 10 mM $NaNO_2$ for 10 min in an electrochemical 10 mL glass cell. After stirring for 10 min, the GCE/CNO electrode was immersed into the mixture, and the potential was cycled between 0 and −0.6 V for 2, 5, 10, 20, 30, 40, 50, or 60 cycles at 0.1 V/s (Scheme 1). The modified electrodes were then sonicated in Milli-Q water for 1 min to remove physically adsorbed compounds. The GC/CNO/PAA and GC/CNO/PM electrodes were studied by cyclic voltammetry (CV) using 1 mM $Fe(CN)_6^{3-/4-}$ in 0.1 M KCl as an electroactive probe. The electrografted PM group was reacted with 500 μM 6-ferrocenylhexanethiol for 2 h, followed by rinsing in acetonitrile. The GC/CNO/PM/Fc electrodes were characterized using CV in 0.1 M tetrabutylammonium tetrafluoroborate in acetonitrile. The surface coverage of Fc was calculated from the area of the anodic peak.

Biosensor Construction and Detection of HPV DNA Sequences. GC/CNO/PAA. The carboxyl groups of PAA were activated with an aqueous mixture of EDC (0.2 M) and NHS (50 mM) for 30 min followed by immersion in 20 μg/mL solution of streptavidin in acetate buffer (pH 5) for 30 min at 4

DOI: 10.1021/acs.analchem.5b00924
Anal. Chem. 2015, 87, 6744−6751

°C. The remaining carboxyl groups were then blocked with 0.1 M ethanolamine hydrochloride (pH 8.5) for 30 min. The electrodes were washed in Milli-Q water and the 5′-biotinylated DNA capture probe (1 μM in Milli-Q water) was incubated for 30 min at room temperature. Afterward, the target DNA (0, 2.5, 5, 10, 20, 50 nM) in Trizma hybridization buffer pH 7.38 was added and incubated for a further 30 min at 37 °C. After washing with Trizma, the HRP-labeled reporter probe (50 nM) was introduced and incubated for another 30 min to complete the DNA sandwich assay.

GC/CNO/PM. A mixture of 1 μM of 5′-thiolated HPV16E7 DNA and 100 μM mercaptohexanol was co-immobilized for 30 min (co-immobilization technique) or modified by sequential incubation of 1 μM thiolated DNA, washed with 0.01 M PBS pH 7.4, and incubated with 100 μM mercaptohexanol (sequential immobilization). Before the addition of the target DNA, the electrodes were washed with 0.1 M PBS pH 7.4. The target DNA and reporter probe were then incubated as described for the PAA surface.

Amperometric measurements were carried out in a 5 mL electrochemical cell containing 0.1 M PBS pH 6 and TMB liquid substrate (2:1 v/v final ratio) under stirring conditions at room temperature. The current was measured at 0.15 V after 2 min for a period of 1 min, and the current vs [DNA] calibration curves were constructed from triplicate measurements. The same modification and detection procedures were employed for GCE/PAA and GCE/PM electrodes as controls.

Clinical samples from cervical scraps, previously genotyped to determine the type of HPV subtype present, were obtained, amplified, and prepared as reported earlier[27] and incubated directly over the electrodes. Electrochemical detection was carried out as described above.

RESULTS AND DISCUSSION

Deposition of CNOs on Glassy Carbon Surfaces. Tip sonication of a CNO suspension in DMF afforded a homogeneous dispersion with an average diameter of 3.7 nm as revealed by TEM (Figure 1a). ESEM analysis of CNOs deposited on GCE after 30 spraying cycles (Figure 1b) indicated that the surface of GCE had been covered with a thin layer of CNOs when compared to the morphology of the bare GCE (not shown) with a thickness of about 9 μm (Figure 1c). The deposited CNO layers showed good mechanical stability, particularly in aqueous solution. Treatments such as repetitive washings with water, immersion in aqueous solutions for a long time, and even sonication for short periods of time did not cause any partial removal of material from the surface of the GCE, as revealed by electrochemical measurements. The morphology of the GC/CNO surface was also studied by AFM (Figure 1d). Round-shaped structures of about 10 nm diameter were observed, consistent with the deposition of CNOs on the surface.

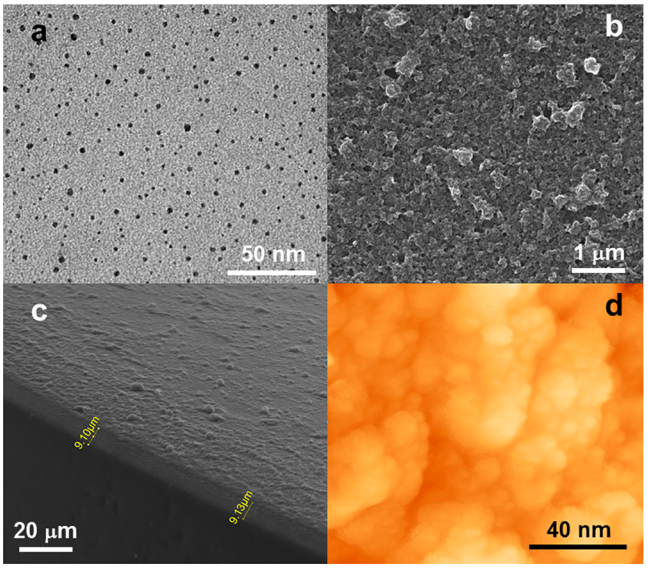

Figure 1. (a) TEM image of dispersed CNOs in DMF after tip sonication. (b,c) ESEM and (d) AFM images of deposited CNO on GC.

Characterization of Diazonium Electrografting on GC/CNO. Phenylacetic acid (PAA). The presence of electrografted PAA moieties on the surface of modified GCE/CNO electrodes was monitored by CV in $Fe(CN)_6^{3-/4-}$ solutions. Carboxylic acid-terminated surfaces are neutral at low pH due to the protonation of the carboxyl group and result in a negative charge as the pH is raised (Scheme 2). Thus, the electrochemical response of the anionic ferricyanide probe is sensitive to pH changes.

Scheme 2. Deprotonation of GC/CNO/PAA in Basic Media

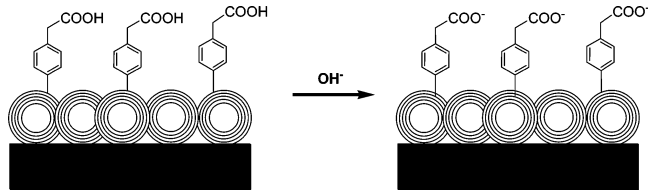

Figure 2a shows variations in the CV response of $Fe(CN)_6^{3-/4-}$ at the surface of modified GCE/CNO/PAA as the pH increases from 1 to 7. As expected, the CV response of $Fe(CN)_6^{3-/4-}$ solutions on modified GCE/CNO/PAA surfaces strongly depends on the pH of the solution. At acidic pH (pH 1), a quasi-reversible redox signal is observed centered at $E_{1/2}$ = 0.28 V and a peak-to-peak separation ΔE = 95 mV, indicating that the surface is essentially neutral and does not effectively block the electron transfer process for the anionic $Fe(CN)_6^{3-/4-}$ probe. As the pH is raised, deprotonation of the COOH groups results in a surface negative that block the probe due to electrostatic repulsion. The dependence of anodic peak current as a function of pH showed an inflection point at pH 2.3, which corresponds to the interfacial pK_a of the modified GCE/CNO/PAA surface (Figure 2b). This value is about 2 orders of magnitude lower than the corresponding value for a GCE/PAA surface (pK_a = 4.7, Figure 2b, inset) and indicates that the presence of the CNO layer enhances the acidity of the PAA, presumably due to the electron withdrawing effect of the polyaromatic CNO structure. This property can be highly advantageous in the design of reactive surfaces as it facilitates its subsequent functionalization.

Phenylmaleimide (PM). The maleimide group has been used as a common cross-linker for the immobilization of thiolated molecules on surfaces.[28] Phenylmaleimide-diazonium was electrografted using cyclic voltammetry on GCE/CNO at different electrodeposition cycles, and the resulting GCE/CNO/PM surface was allowed to react with Fc-SH and

DOI: 10.1021/acs.analchem.5b00924
Anal. Chem. 2015, 87, 6744−6751

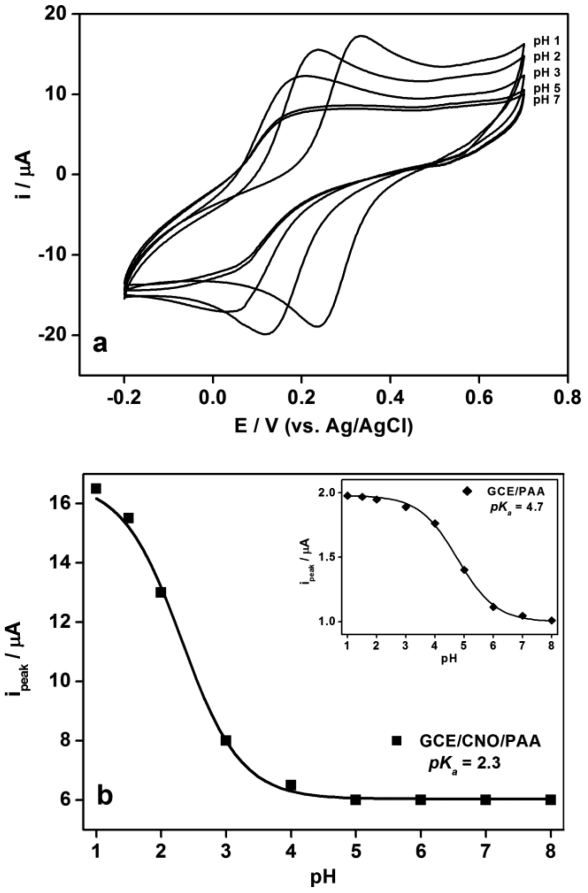

Figure 2. (a) Cyclic voltammograms (for 1 mM $K_3Fe(CN)_6$ in 0.1 M KCl at 0.1 V s^{-1}) obtained at different pH values on a GCE/CNO/PAA electrode. (b) Titration curve corresponding to the variations of the anodic peak intensity. The solid line was obtained by fitting the experimental points to a sigmoidal curve. Inset: Corresponding titration curve for GCE/PAA.

characterized by CV in 0.1 M tetrabutylammonium tetrafluoroborate in acetonitrile (Scheme 3).

Scheme 3. Reaction of GC/CNO/PM with Fc-SH

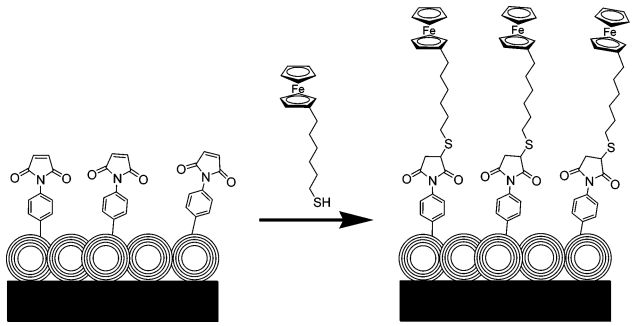

Figure 3a shows the values of surface coverage of ferrocene (Γ_{FcSH}) at different electrodeposition cycle numbers calculated from the area of the oxidation wave. Γ_{FcSH} values increased steadily with the number of potential cycles until a maximum of 2.4×10^{-9} mol/cm^2 was obtained after 30 cycles. A similar tendency was observed for the GCE/PM surface, but in this case the maximum surface coverage obtained was 0.7×10^{-9} mol/cm^2, also after 30 cycles. This marked difference in Γ_{FcSH} values can be explained by considering that the CNOs increase

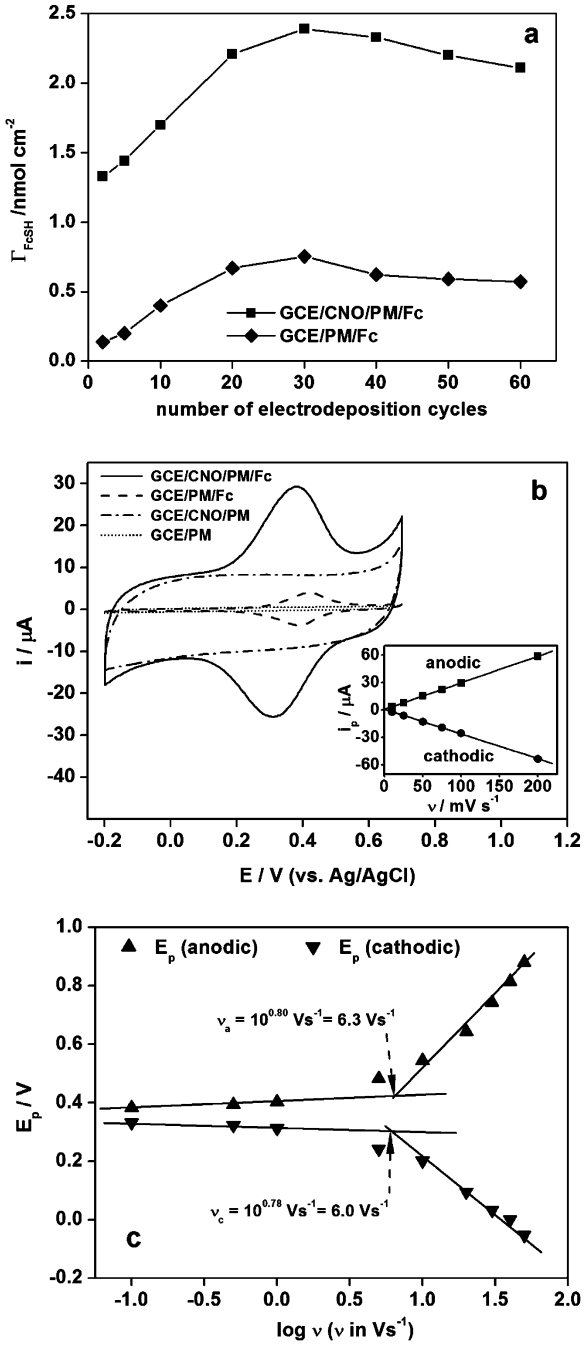

Figure 3. (a) Dependence of Γ_{FcSH} with the number of electrodeposition cycles. (b) Cyclic voltammograms of PM-modified surfaces in 0.1 M TBA-TFB in acetonitrile at 0.1 V s^{-1} (inset: plot of peak currents vs scan rate for GCE/CNO/PM/Fc. (c) Dependence of E_p with log ν determined from cyclic voltammograms for GCE/CNO/PM/Fc.

the effective surface active area of the electrodes making more PM molecules available for interaction with FcSH, which results in an enhancement of the current intensity of the electroactive species relative to the GCE-based electrode.

Figure 3b shows a comparison of the CV obtained for bare and Fc modified surfaces in the presence and absence of CNOs after 30 electrodeposition cycles in TBA-TFB. The peaks are essentially symmetrical with a peak-to-peak separation ΔE_{ac} = 66 mV for GCE/PM/CNO/Fc. ΔE_{ac} is essentially scan rate-independent up to 1 V/s, and the peak currents depend linearly

DOI: 10.1021/acs.analchem.5b00924
Anal. Chem. 2015, 87, 6744−6751

with the scan rate, indicating that the Fc groups are surface-confined. Interestingly, for the CNO-modified surface, the Fc signal is not only larger than for the GCE/PM/Fc surface but also appears shifted 61 mV to lower potentials. Figure 3c shows the dependence of the peak potential (E_p) with log ν, where ν is the scan rate, determined by CV. Using Laviron's formalism,[29] the apparent rate constant for electron transfer (k) can be calculated from the equation

$$k = \alpha n F \nu_c / RT = (1 - \alpha) n F \nu_a / RT$$

where α is the transfer coefficient calculated from the quotient $\nu_a/(\nu_c + \nu_a)$, ν_c and ν_a are the limiting cathodic and anodic scan rates obtained from Figure 3c, and F is Faraday's constant. Under these conditions, $\alpha = 0.51$ and $k = 122\ s^{-1}$ for the GCE/PM/CNO/Fc system, while $k = 19\ s^{-1}$ in the absence of CNO indicating a markedly faster electron transfer rate when the CNOs are present.

Amperometric Detection of DNA on CNO-Modified Electrodes. The possibility to use CNO-modified surfaces in the detection of biomolecules was tested using DNA sequences associated with the human papillomavirus (HPV) as a model system. PAA- and PM-grafted CNO surfaces were modified with a recognition DNA sequence, and a sandwich type assay was used to detect the target sequence using a peroxidase-labeled DNA reporter probe in both cases. The assay conditions used were similar to those previously reported by our group for the detection of HPV sequences on thiol-modified gold electrodes.[26,27]

Scheme 4 shows the strategy used for the attachment of the DNA recognition sequence to the GC/CNO/PAA surface. The COOH groups of the surface were activated using carbodiimide chemistry followed by covalent immobilization of streptavidin and incubation of a biotinylated DNA capture probe. Figure 4a

Scheme 4. (a) EDC/NHS, (b) Streptavidin, (c) Ethanolamine, (d) Biotinylated HPV16 Capture Probe, (e) Target Sequence, and (f) HRP-DNA Detecting Sequence

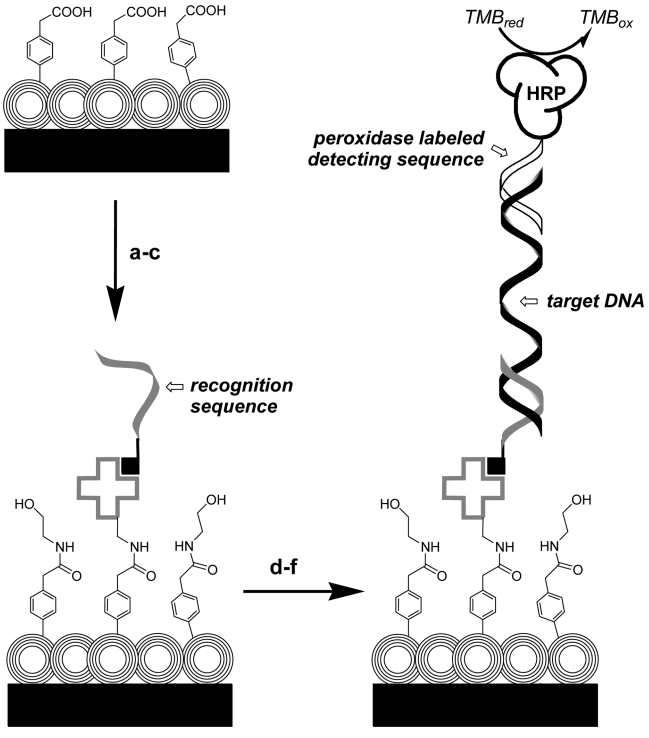

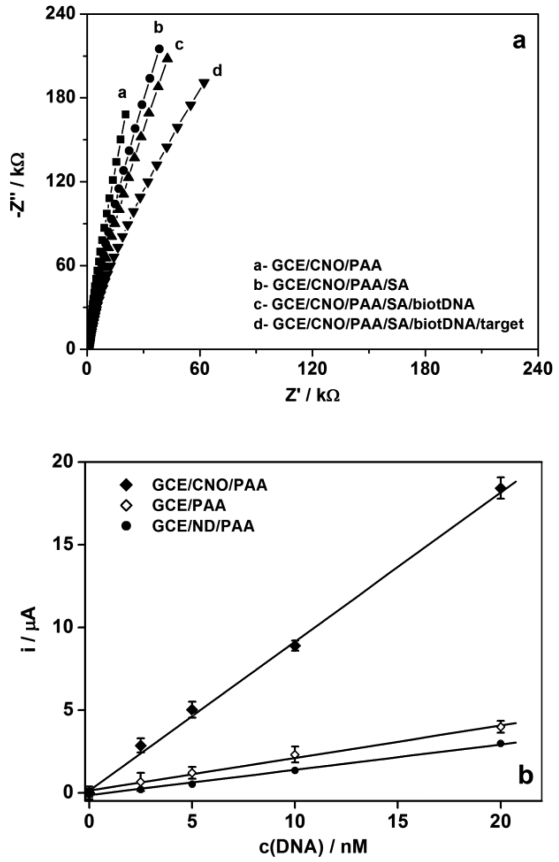

Figure 4. (a) Complex impedance plots (in 1 mM $K_3Fe(CN)_6$ in phosphate buffer pH 7.4) corresponding to the sequential immobilization of streptavidin, biotinylated DNA, and target DNA (10 nM) on GCE/CNO/PAA electrodes. (b) Calibration curves for the detection of target DNA on GCE, GCE/CNO, and GC/ND electrodes modified with PAA.

shows the AC impedance responses for $Fe(CN)_6^{3-/4-}$ as a function of the construction steps of the biosensor. The Nyquist plots obtained for every step show high slopes, typical of a capacitive behavior. The sequential immobilization of streptavidin, biotinylated DNA, and target DNA was accompanied by a successive increase in the resistance to charge transfer from 133 to 315 Ω, indicating a blocking of the electron transfer of the probe upon addition of the different layers. This demonstrates the successful formation of the sensing layer on the CNO-modified GCE.

Figure 4b shows the variation of current intensity with DNA concentration in the presence and in the absence of CNO for PAA-terminated electrodes. For the GCE/CNO/PAA surface, the calibration curve shows a markedly better sensitivity (0.91 $\mu A\ nM^{-1}$) and a lower limit of detection (0.54 nM) as compared with the control surface in the absence of CNO (sensitivity = 0.21 $\mu A\ nM^{-1}$; LOD = 3.9 nM). This is 4.3-fold sensitivity increase and a factor of 7 reduction in LOD after the incorporation of CNOs on the surface. Interestingly, no sensitivity increase was observed when the CNO layer was replaced by one prepared with the precursor nanodiamonds (ND), indicating that the CNOs play a key role in the observed improvement of the analytical response (Figure 4b).

In the case of the GC/CNO/PM surface, a thiolated DNA capture probe was reacted with the immobilized maleimide group to form a stable thioether bond (Scheme 5). Figure 5a

DOI: 10.1021/acs.analchem.5b00924
Anal. Chem. 2015, 87, 6744−6751

Scheme 5. (a) Thiolated HPV16 Capture Probe/Mercapto-hexanol, (b) Target Sequence, (c) HRP-DNA Probe

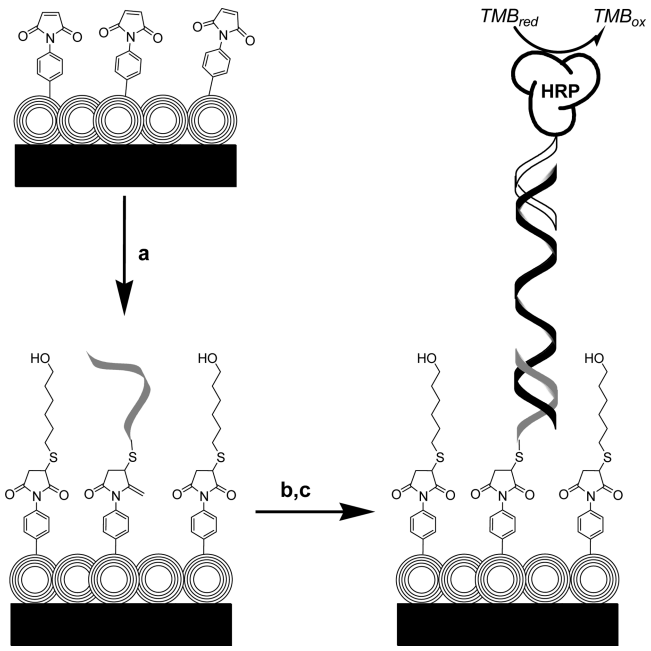

shows a comparison of the currents obtained for the detection of 5 and 20 nM target sequence using either a co-immobilization strategy (thiolaled HPV16 capture probe mixed with mercaptohexanol in 1:100 molar ratio) or sequential addition of thiolated probe and mercaptohexanol in the same molar ratio.[30] As shown, the co-immobilization strategy gives a 2-fold higher signal as compared to backfilling and is in agreement with previous results reported for the co-immobilization of thiolated DNA probes with mercaptohexanol on gold surfaces. This result also suggests that the co-immobilization strategy may be generalized to other surfaces and, therefore, was used for the construction of the CNO-based sensor.

Figure 5b presents the amperometric detection of different target DNA concentrations for both GCE/CNO/PM and GCE/PM electrodes. The calibration curve for GCE/CNO/PM has a slope of 0.41 μA nM^{-1} with a limit of detection of 0.50 nM as compared with the control surface without CNOs (sensitivity = 0.11 μA nM^{-1}; LOD = 1.4 nM). This represents a 4-fold sensitivity increase and a factor of 3 reduction in LOD after the incorporation of CNOs on the surface. In addition, the CNO-based sensors showed a markedly larger linear range (0–20 nM) and sensitivity as compared to the thiol-based immobilization on gold (0–1 nM, 0.15 μA nM^{-1}).[26] The CNO-based genosensor was evaluated with four clinical samples obtained from cervical scraps previously genotyped to assess the absence or presence of HPV subtypes 16, 18, and 45. As shown in Figure 5c, an excellent correlation with the HPV genotyping was obtained as evidenced by the markedly higher signal obtained for the sample containing HPV16, as expected considering that the GCE/CNO/PM genosensor was modified with a thiolated probe selective to HPV16.

As shown, the presence of CNOs on the surface enhanced the sensitivity and lowered the limits of detection of the amperometric assays with respect to the GC-only electrodes. This result is primarily due to the larger surface area achieved in the presence of CNO, which allows a much higher number of

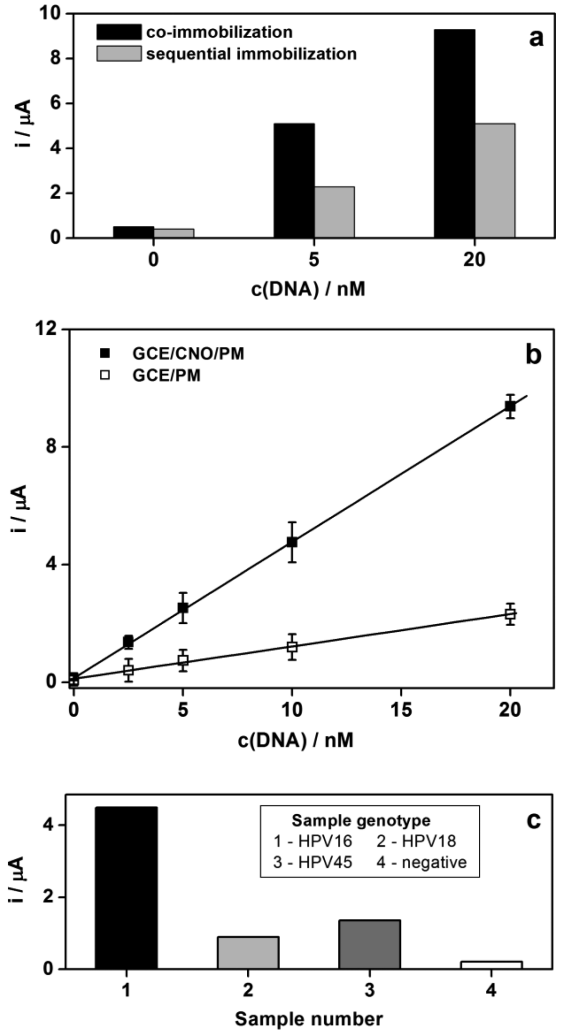

Figure 5. (a) Comparison of the currents obtained during the detection of 5 and 20 nM target sequence using co-immobilization and sequential addition of thiolated probe and mercapto-hexanol in 1:100 molar ratio. (b) Calibration curves for the detection of target DNA on GCE and GCE/CNO electrodes modified with PM using the co-immobilization strategy. (c) Current values obtained from undiluted clinical samples on the GC/CNO/PM genosensor modified with an HPV16 capture probe. The HPV subtype of each sample is indicated in the inset.

recognition sequences to be immobilized on the surface. Another factor to be considered is the electron transfer rate of TMB on the CNO-modified surface. It is known that TMB undergoes a quasi-reversible two-proton coupled two-electron redox process in acidic pH. Inspection of the CV of TMB at the GC/CNO surface (Figure 6) shows a large current enhancement associated with the increase in surface area. In addition, the CV response shows a marked displacement (−90 mV) toward less positive potentials with respect to the GC-only system, indicating a faster electron transfer, in accord with the results obtained on the GC/CNO/PM/Fc surface. In our case, this favored electron transfer effect is larger than that recently observed for catechol-based neurotransmitters,[31] which were ascribed to the semi-metal properties and to the presence of structural defects on the CNOs that enhance electron transfer properties.[32] Thus, the combination of the unique morphological and electronic properties provided by the CNOs to the GC surfaces enhance the sensitivity of the assay and opens the

DOI: 10.1021/acs.analchem.5b00924
Anal. Chem. 2015, 87, 6744–6751

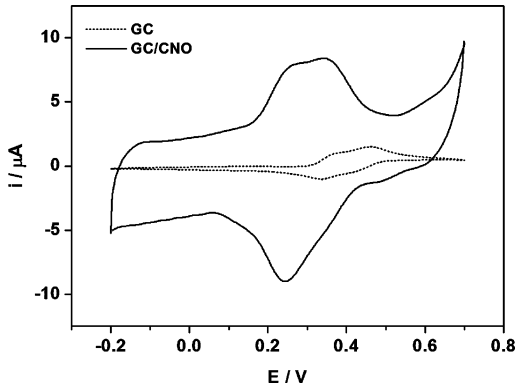

Figure 6. Cyclic voltammograms recorded in 0.1 M PBS pH 6 containing 0.1 mM TMB hydrochloride on GC and GC/CNO surfaces. ν = 0.1 V s^{-1}.

way for further applications of CNO-based surfaces for the detection of other biomolecules. Such studies are currently underway.

CONCLUSIONS

Carbon nano-onion dispersions were deposited on the surfaces of glassy carbon electrodes, and the modified surfaces were studied by ESEM and AFM revealing a relatively uniform surface. The glassy carbon electrodes modified with CNOs were further modified by electrografting of diazonium salts possessing carboxylic acid or maleimide groups. The attachment of phenyl acetic acid to GCE/CNO generated a COOH-terminated surface to which streptavidin and biotinylated capture DNA sequence was immobilized. On the other hand, the maleimide-terminated surfaces were used for the capture of a thiolated DNA probe, and both sensing platforms were investigated for the detection of a DNA sequence associated with the human papillomavirus. In both cases, the incorporation of CNOs on the surface resulted in better sensitivities and lower limits of detection as compared to a GCE electrode without the CNOs. These results were explained on the basis of the large surface area combined with enhanced electron transfer properties of the CNO-modified electrodes. These observations suggest that the developed CNO-modified surfaces are promising and versatile candidates for the development of different and effective analytical sensor systems.

AUTHOR INFORMATION

Corresponding Authors

*E-mail echegoyen@utep.edu (L. E.).
*E-mail alex.fragoso@urv.cat (A. F.).

Notes

The authors declare no competing financial interest.

ACKNOWLEDGMENTS

J.P.B. thanks the Departament d'Enginyeria Química of Universitat Rovira i Virgili for a predoctoral scholarship. Financial support from Ministerio de Economía y Competitividad, Spain (Grant BIO2012-30936 to A.F.), is gratefully acknowledged. L.E. thanks the National Science Foundation (Grant CHE-1408865) and the Robert A. Welch Foundation (endowed chair, Grant AH-0033) for generous support for this work.

REFERENCES

(1) Ugarte, D. *Nature* **1992**, *359*, 707−709.
(2) Sano, N.; Wang, H.; Chhowalla, M. *Nature* **2001**, *414*, 506−507.
(3) Echegoyen, L.; Ortiz, A.; Chaur, M. N.; Palkar, A. J. Carbon Nano Onions. In *Chemistry of Nanocarbons*; Akasaka, T., Wudl, F., Nagase, S., Eds.; John Wiley & Sons: Chichester, U.K., 2010; pp 463−483.
(4) Bartelmess, J.; Giordani, S. *Beilstein J. Nanotechnol.* **2014**, *5*, 1980−1998.
(5) Georgakilas, N.; Guldi, D. M.; Signorini, R.; Bozio, R.; Prato, M. *J. Am. Chem. Soc.* **2003**, *125*, 14268−14269.
(6) Rettenbacher, A. S.; Elliott, B.; Hudson, J. S.; Amirkhanian, A.; Echegoyen, L. *Chem.—Eur. J.* **2006**, *12*, 376−387.
(7) Sek, S.; Breczko, J.; Plonska-Brzezinska, M. E.; Wilczewska, A. Z.; Echegoyen, L. *ChemPhysChem* **2013**, *14*, 96−100.
(8) Borgohain, R.; Li, J.; Selegue, J. P.; Cheng, Y.-T. *J. Phys. Chem. C* **2012**, *116*, 15068−15075.
(9) Flavin, K.; Chaur, M. N.; Echegoyen, L.; Giordani, S. *Org. Lett.* **2010**, *12*, 840−843.
(10) Palkar, A.; Kumbhar, A.; Athans, A. J.; Echegoyen, L. *Chem. Mater.* **2008**, *20*, 1685−1687.
(11) Wajs, E.; Molina-Ontoria, A.; Nielsen, T. T.; Echegoyen, L.; Fragoso, A. *Langmuir* **2015**, *31*, 535−541.
(12) Macutkevic, J.; Adomavicius, R.; Krotkus, A.; Seliuta, D.; Valusis, G.; Maksimenko, S.; Kuzhir, P.; Batrakov, K.; Kuznetsov, V.; Moseenkov, S.; Shenderova, O.; Okotrub, A. V.; Langlet, R.; Lambin, P. *Diamond Relat. Mater.* **2008**, *17*, 1608−1612.
(13) Breczko, J.; Winkler, K.; Plonska-Brzezinska, M. E.; Villalta-Cerdas, A.; Echegoyen, L. *J. Mater. Chem.* **2010**, *20*, 7761−7768.
(14) Breczko, J.; Plonska-Brzezinska, M. E.; Echegoyen, L. *Electrochim. Acta* **2012**, *72*, 61−67.
(15) Pech, D.; Brunet, M.; Durou, H.; Huang, P.; Mochalin, V.; Gogotsi, Y.; Taberna, T.-L.; Simon, P. *Nat. Nanotechnol.* **2010**, *5*, 651−654.
(16) Joly-Pottuz, L.; Bucholz, E. W.; Matsumoto, N.; Phillpot, S. R.; Sinnott, S. B.; Ohmae, N.; Martin, J. M. *Tribol. Lett.* **2010**, *37*, 75−81.
(17) Keller, N.; Maksimova, N. I.; Roddatis, V. V.; Schur, M.; Mestl, G.; Butenko, Y. V.; Kuznetsov, V. L.; Schlögl, R. *Angew. Chem., Int. Ed.* **2002**, *41*, 1885−1888.
(18) Bartelmess, J.; Quinn, S. J.; Giordani, S. *Chem. Soc. Rev.* **2015**, DOI: 10.1039/C4CS00306C.
(19) Ghosh, M.; Sonkar, S. K.; Saxena, M.; Sarkar, S. *Small* **2011**, *7*, 3170−3177.
(20) Bartelmess, J.; De Luca, E.; Signorelli, A.; Baldrighi, M.; Becce, M.; Brescia, R.; Nardone, V.; Parisini, E.; Pompa, P. P.; Echegoyen, L.; Giordani, S. *Nanoscale* **2014**, *6*, 13761−13769.
(21) Yang, M.; Flavin, K.; Radics, G.; Hearnden, C. H. A.; McManus, G. J.; Moran, B.; Villalta-Cerdas, A.; Echegoyen, L.; Giordani, S.; Lavelle, E. C. *Small* **2013**, *9*, 4194−4206.
(22) Luszczyn, J.; Plonska-Brzezinska, M. E.; Palkar, A.; Dubis, A. T.; Simionescu, A.; Simionescu, D. T.; Kalska-Szostko, B.; Winkler, K.; Echegoyen, L. *Chem.—Eur. J.* **2010**, *16*, 4870−4880.
(23) Yáñez-Sedeño, P.; Riu, J.; Pingarrón, J. M.; Rius, F. X. *TrAC, Trends Anal. Chem.* **2010**, *29*, 939−953.
(24) Yang, W.; Ratinac, K. R.; Ringer, S. P.; Thordarson, P.; Gooding, J. J.; Braet, P. *Angew. Chem., Int. Ed.* **2010**, *49*, 2114−2138.
(25) Thomison, J.; Thomas, L. K.; Shroyer, K. R. *Hum. Pathol.* **2008**, *39*, 154−166.
(26) Civit, L.; Fragoso, A.; O'Sullivan, C. K. *Electrochem. Commun.* **2010**, *12*, 1045−1048.
(27) Civit, L.; Fragoso, A.; Hölters, S.; Dürst, M.; O'Sullivan, C. K. *Anal. Chim. Acta* **2012**, *715*, 93−98.
(28) Hermanson, G. T. *Bioconjugate Techniques*, 2nd ed.; Academic Press: New York, 2008; Chapter 19.
(29) Laviron, E. *J. Electroanal. Chem.* **1979**, *101*, 19−28.
(30) Henry, O. Y. F.; Gutierrrez Pérez, J.; Acero Sánchez, J. L.; O'Sullivan, C. K. *Biosens. Bioelectron.* **2010**, *25*, 978−983.
(31) Borgohain, R.; Yang, J.; Selegue, J. P.; Kim, D. Y. *Carbon* **2014**, *66*, 272−284.

DOI: 10.1021/acs.analchem.5b00924
Anal. Chem. 2015, 87, 6744−6751

(32) Ueda, A.; Kato, D.; Kurita, R.; Kamata, T.; Inokuchi, H.; Umemura, S.; Hirono, S.; Niwa, O. *J. Am. Chem. Soc.* **2011**, *133*, 4840−4846.

DOI: 10.1021/acs.analchem.5b00924
Anal. Chem. 2015, 87, 6744−6751